International Journal of Applied Engineering Research ISSN 0973-4562 Volume 13, Number 18 (2018) pp. 13677-13682
© Research India Publications. http://www.ripublication.com

Magnetism of low concentration MT (MT = Ti, V, Cr)-doped AlN zincblende density functional theory study

Miguel J. Espitia R[1], John H. Díaz F[1], Octavio José Salcedo Parra[2,3]

[1]*GEFEM Group, Universidad Distrital "Francisco José de Caldas", Bogotá, Colombia.*

[2]*Internet Inteligente Research Group, Universidad Distrital "Francisco José de Caldas", Bogotá, Colombia.*

[3]*Faculty of Engineering - Universidad Nacional de Colombia, Bogotá D.C., Colombia.*

Abstract

First-principles calculations within the framework of density functional theory were carried out in order to study the structural, electronic, and magnetic properties of the $Al_{0.0625}MT_{0.9375}N$ (MT = Ti, V and Cr) compounds in the zincblende structure. The calculations were done with the pseudopotential method, employing computational Quantum ESPRESSO code. A study of the density of states showed that the $Al_{0.0625}Ti_{0.9375}N$ compound has a metallic character, while $Al_{0.0625}V_{0.9375}N$ and $Al_{0.0625}Cr_{0.9375}N$ exhibit a half-metallic behavior. The total magnetic moments of $Al_{0.0625}Ti_{0.9375}N$, $Al_{0.0625}V_{0.9375}N$, and $Al_{0.0625}Cr_{0.9375}N$ were 0.85 μ_β, 2.0 μ_β, and 3.0 μ_β per cell, respectively, mainly being contractions of the total magnetic moment of the 3d-MT orbital, with a minimum contribution from its four nearest neighbors, the 2p-N states. The results suggest that, AlN doped with V and Cr is a promising candidate to be a good diluted magnetic semiconductor material.

Keywords: Half-metallic ferromagnetism, diluted magnetic semiconductor, electronic and magnetic properties.

INTRODUCTIÓN

Due to its applications in the spintronic field, the diluted magnetic semiconductors (DMS) materials has been attracted great scientific interest because are good candidates for microelectronic applications, where the load and the spin are exploited simultaneously. Several advantages of the spintronic are expected with respect to conventional electronics, for example: nonvolatility, low power consumption, high data processing speed and increased transistor density. Among the III-V, the Aluminum nitride (AlN) has been extensive studied due to use in spintronics. The AlN has the largest energy band, 6.2 eV of the III nitrides. The AlN have high thermal stability, high melting point, high thermal conductivity, large bulk module, high chemical stability, very strong bond strength, and low compressibility. Due to these properties and with its large band-gap energy AlN has potential technological applications for high-temperature transistors, light-emitting diodes (LEDs) in the violet, blue, and green regions, lasers, and optical detectors [1, 2, 3]. Actually, AlN is widely used in the semiconductor industry, and many of its potential applications are a reality. Some electronic and optoelectronic devices are now available commercially [4], such as green [5] and blue [6] LEDs and lasers [7]. Additionally, in recent years several theoretical investigations [8–17] and experimental studies [18–27] have found that AlN doped with transition metals (TM) [28–30] turned out to be a good diluted magnetic semiconductor for use in spintronics devices. All these studies of TM-doped AlN were made in the wurtzite structure, because the wurtzite phase is the ground state of AlN. however, recently there has been a lot of interest in AlN in the zincblende structure, because AlN-zincblende has been grown by different experimental techniques, such as solid-state reaction [31], molecular beam epitaxy MBE [4], the vapor–liquid–solid (VLS) route [32], and reactive pulsed laser deposition [33]. Though it is expected that AlN zincblende applications will be similar to those developed for AlN wurtzite, many researchers have found several advantages of the zincblende over the wurtzite structure [34–36], because the zincblende phase of AlN doesn't have a polarized internal electric field [37], due to its high crystallographic symmetry. The absence of an internal electric field in AlN zincblende improves its electronic properties, because of higher carrier mobility, higher drift velocities, and better doping efficiencies [34–36]. At the same time, there are additional advantages for group-III semiconductors in the cubic phase; for example, in GaN zincblende its was found that there is a reduction in the radiative radiation time by two orders of magnitude compared to GaN wurtzite [38]. In spite of cubic AlN have better performance and the technological developments for the growth of AlN in zincblende structure are now available, from the theoretical point of view, zincblende AlN doped with Ti, V, and Cr has not been studied sufficiently. In this paper, we focus our study in the structural, electronic, and magnetic properties of AlN zincblende doped with MT = Ti, V, Cr in the concentrations of $Al_{0.0625}Ti_{0.9375}N$, $Al_{0.0625}V_{0.9375}N$ and $Al_{0.0625}Cr_{0.9375}N$, due to huge potential applications.

COMPUTATIONAL METHOD

We performed *ab*-initio calculations using full-potential linearized augmented plane wave (FP-LAPW) method within the framework density functional theory (DFT) [11, 12] as implemented in the Wien2k computational code [13]. The correlation and exchange energies were included with the generalized gradient approximation (GGA) of Perdew, Burke, and Ernzerhof (PBE) [14]. The basis function was expanded up to cutoff parameter of $R_{MT}*K_{max} = 8$ (R_{MT} is the smallest radius of the atomic level within the unit cell and K_{max} is the magnitude of the largest k vector of the reciprocal lattice). Brillouin zone integrations were performed with the special k-point method over a 140 Monkhorst-Pack mesh [15]. For the expansion of the potential in the interstitial region between muff-tin spheres, $G_{max} = 12$ was considered. The spherical harmonics for the charge density was expand up to $l_{max} = 10$ inside the atomic spheres. The radii muff-tin of the atoms were 1.6, 1.8, and 2.0 bohr, for N, Al, and Cr respectively. All the calculations were performed with spin polarization. To simulate the ternary wurtzite alloys, we employ 8-atoms supercell for $Al_{0,25}Cr_{0.75}N$ and $Al_{0,75}Cr_{0.25}N$, corresponding to 1x1x2 conventional wurtzite cell, while the $Al_{0,50}Cr_{0.50}N$ we are using the 4-atoms supercell, corresponding to 1x1x1 conventional wurtzite cell, as show fig. 1. The optimization process ended when the forces became smaller than 10^{-4} eV/Å. The convergence threshold for self-consistent field iteration was 10^{-5} eV.

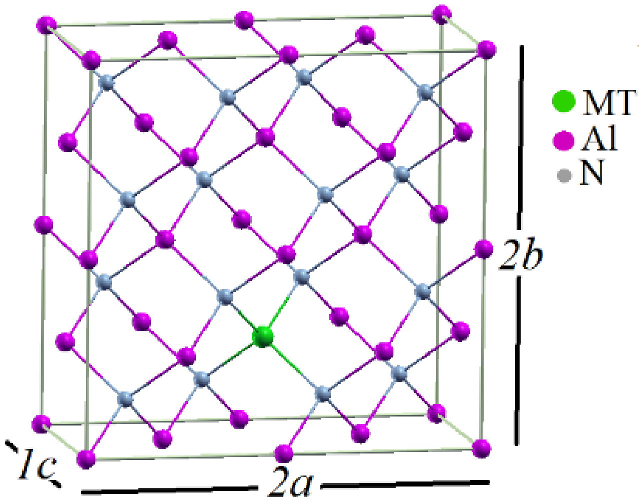

Figure 1. Conventional unit cell of pure AlN in the zincblende structure. Source: Authors

RESULTS AND DISCUSSIONS

Structural properties

To evaluate the structural parameters such as lattice constant (a_0), bulk modullus (B_0) and, total energy (E_0) of the pristine AlN, $Al_{0.0625}Ti_{0.9375}N$, $Al_{0.0625}V_{0.9375}N$ and $Al_{0.0625}Cr_{0.9375}N$ in the zincblende structure, we performed minimization process of the total energy using vc-relax calculations. all calculations were carry out with spin-polarized. Additionally, in order to determine the magnetic phase most stable for the $Al_{0.125}V_{0.875}N$ compound the ferromagnetic (FM) and antiferromagnetic (AFM) phases were calculated, several AFM configurations with different spin orientations were considered until obtaining the most stable structure.

Table 1: Calculated lattice constant and bulk modulus$Al_{0.0625}V_{0.9375}N$, and $Al_{0.125}V_{0.875}N$ in the zincblende structure, together with recently reported theoretical and experimental values

Compound	a(Å)	B_0 (GPa)
Pristine-AlN	4.3815	206.52
	4.3800[a]	212.70[b]
	4.3790[c]	211.78[d]
	4.3700[e]	202.00[e]
$Al_{0.0625}Ti_{0.9375}N$	4.3886	186.98
$Al_{0.0625}V_{0.9375}N$	4.3710	185.83
$Al_{0.0625}Cr_{0.9375}N$	4.3624	190.13

[a] Theoretical Reference [46].

[b] Theoretical Reference [47].

[c] Theoretical Reference [48].

[d] Theoretical Reference [49].

[e] Experimental Reference [50].

In the table 1 are listed the resulting the equilibrium lattice constant, bulk modullus and total minimum energy along with experimental and theoretical recent reported. We obtained for the lattice constant 4.3815 Å for AlN-zincblende, in comparison with the experimental value 4.3700 Å [50], the error in lattice constant was ~ 0.263%, while the maximum discrepancy with value reported theoretically. 4.3790 Å [48] was ~ 0.13%. In both cases, the difference is less than 1%. Therefore, the calculated lattice constant pure AlN-zincblende is in very good agreement with reported experimental and theoretically values. For the calculated value of the bulk modullus, 206.52 GPa the error in comparison with experimental value 202.00 GPa [50] was ~ 2.23%. We observed that the value of the calculated bulk modulus here is closer to the experimental value than those reported by other authors; hence the values reported for the lattice constant and the bulk modulus are acceptable.

We note that in the $Al_{0.0625}Ti_{0.9375}N$, $Al_{0.0625}V_{0.9375}N$ and $Al_{0.0625}Cr_{0.9375}N$ compounds, the equilibrium lattice constant changes with respect to pristine AlN-zincblende. For $Al_{0.0625}Ti_{0.9375}N$, the lattice constant increases slightly, because the atomic radius of the Ti atom (1.47 Å) is slightly larger than that of Al (1.43 Å), while for the $Al_{0.0625}V_{0.9375}N$ and $Al_{0.0625}Cr_{0.9375}N$ compounds, the lattice constant decreases, because the atomic radius of Al is larger than that of the V and Cr atoms. The largest decrease in the lattice constant is for the $Al_{0.0625}Cr_{0.9375}N$ compound, because the atomic radius of Cr (1.27 Å) is smaller than that of the Al atom.

In order to check the relative stability for $Al_{0.0625}Ti_{0.9375}N$, $Al_{0.0625}V_{0.9375}N$ and $Al_{0.0625}Cr_{0.9375}N$ in the zincblende structure, we estimate the formation energy for each concentration, the formation energy is definite as [30]:

$$E_f = E_{MT:AlN} - E_{AlN} - mE_{MT} + mE_{Al}$$

Where, $E_{MT:AlN}$, E_{AlN}, E_{MT} and E_{Al} are the total energies of MT (MT = Ti, V, Cr)-doped AlN, pristine AlN zincblende, MT in its corresponding ground state and fcc-Al. *m* is the number of MT atoms that occupy the positions of the Al atoms, in this case $m = 1$. The calculated values of the formation energy for a single MT doped AlN zincblende, namely, $Al_{0.0625}Ti_{0.9375}N$, $Al_{0.0625}V_{0.9375}N$ and $Al_{0.0625}Cr_{0.9375}N$ concentration was 2.215 eV, 2.712 eV and 4.658 eV, respectively. When comparing the formation energy of $Al_{0.0625}V_{0.9375}N$ and $Al_{0.0625}Cr_{0.9375}N$ in the zincblende structure calculated here with the formation energy in the wurtzite structure of 2.49 eV [51] and 4.41 eV [52], respectively, we observe that they are close, for this reason and the moderate values for formation energy of $Al_{0.0625}Ti_{0.9375}N$, $Al_{0.0625}V_{0.9375}N$ and $Al_{0.0625}Cr_{0.9375}N$ compounds indicate that can be easily grown.

Electronic Properties

The band structure and spin-polarized density of states (DOS) along the symmetry path of pristine AlN and $Al_{0.0625}MT_{0.9375}N$ (MT = Ti, V, Cr) in the zincblende structure were calculated with the equilibrium lattice constant show in table 1. The band structure and DOS are shown in the fig. 2 and fig 3, respectively. Where we have chosen the Fermi Level as zero of energy.

In Fig. 2(a), we can see that pristine AlN-zincblende is an indirect band gap semiconductor material, with the top of the valence band located at the X point and the bottom of the conduction band located at the Γ point of the Brillouin zone. The calculated value of energy band is 3.37 eV, which is very close to previous theoretical results 3.38 eV [53], 3.40 eV [54] and 3.36 eV [55].

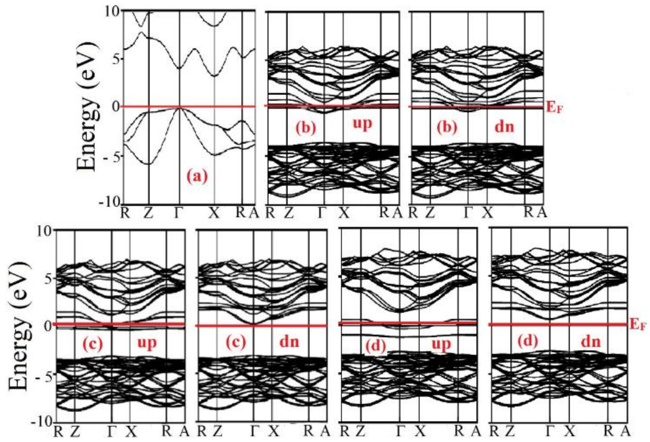

Figure 2. Band structure in the zincblende phase of (a) pristine AlN, (b) $Al_{0.0625}Ti_{0.9375}N$, (c) $Al_{0.0625}V_{0.9375}N$, (d) $Al_{0.0625}Cr_{0.9375}N$. Source: Authors

Fig. 2(c)-(d) shows the spin up and spin down band structure of the $Al_{0.0625}Ti_{0.9375}N$, $Al_{0.0625}V_{0.9375}N$, and $Al_{0.0625}Cr_{0.9375}N$ concentrations. The band structure for $Al_{0.0625}Ti_{0.9375}N$ shows a metallic behavior, because the two spin channels cross the fermi level, while the band structure of the $Al_{0.0625}V_{0.9375}N$ and $Al_{0.0625}Cr_{0.9375}N$ compounds reveals a half-metallic character, with the spin down being semiconducting and the spin up being metallic. We can see in Figures 2(c) and 2(d) that above the Femi level the band structure has a dispersed band. Due to the spin up orientation's being partially filled, there are sufficient states behaving like free holes. Consequently, these compounds have 100% spin polarization of the conduction carriers and satisfy this requirement for use as spin injectors [56-58].

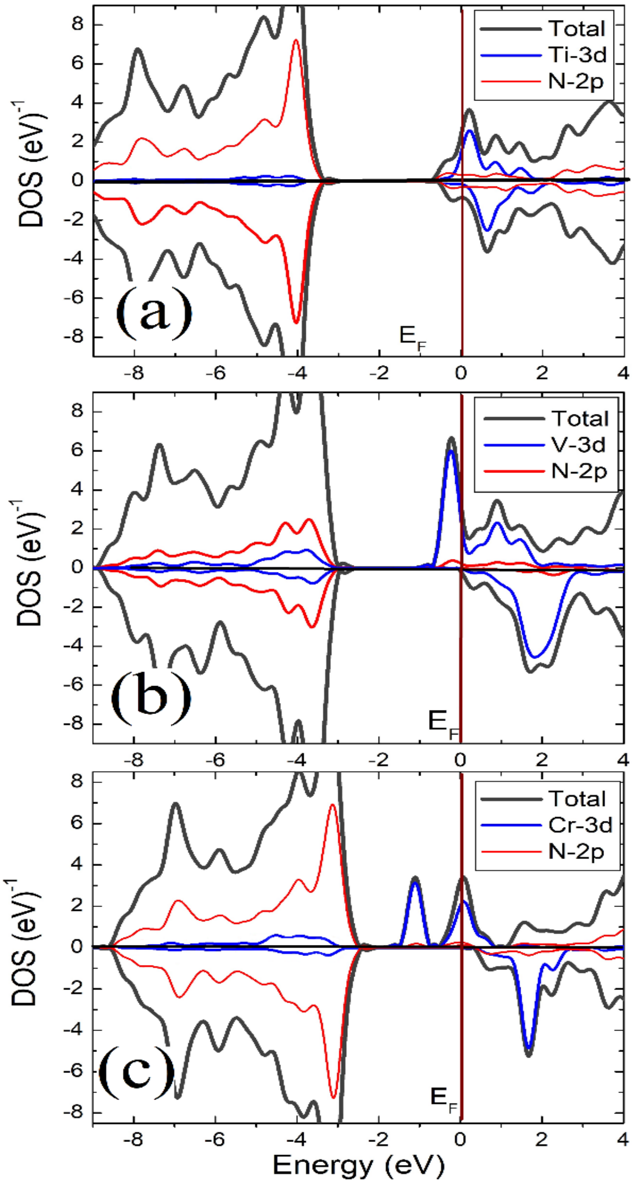

Figure 3. Total and partial density of states of ternary compound (a) $Al_{0.0625}Ti_{0.9375}N$, (b) $Al_{0.0625}V_{0.9375}N$, (c) $Al_{0.0625}Cr_{0.9375}N$. Source: Authors

In Fig. 3(a)-(c), the DOS of $Al_{0.0625}Ti_{0.9375}N$, $Al_{0.0625}V_{0.9375}N$, and $Al_{0.0625}Cr_{0.9375}N$ can be seen. With the DOS of $Al_{0.0625}Ti_{0.9375}N$, it is verified once more that this compound exhibits a metallic behavior, because both spin up and spin down cross the Fermi level, while for $Al_{0.0625}V_{0.9375}N$ and $Al_{0.0625}Cr_{0.9375}N$, the DOS again shows their half-metallic character, because only the spin channel (spin up) crosses the Fermi level. The DOS of the three compounds shows that the spin density is mainly situated around the MT atom, with a minimum contribution from the first-neighboring N atoms. For this reason, near the Fermi level the main contribution to the total DOS comes from the 3d-MT (MT = Ti, V, Cr) orbital, with a minimum contribution from the 2p-N orbital. The hybridization and the polarization between 3d-V and 2p-N generate AlN, $Al_{0.0625}Ti_{0.9375}N$, $Al_{0.0625}V_{0.9375}N$ and $Al_{0.0625}Cr_{0.9375}N$ compounds with a finite magnetic moment, with values of 0.85 μ_β, 2.0 μ_β, and 3.0 μ_β per cell. The values of the magnetic moment of $Al_{0.0625}V_{0.9375}N$ and $Al_{0.0625}Cr_{0.9375}N$ are integers; this confirms the half-metallic ferromagnetic character of the compounds. We can see in the DOS figure that the magnetic moment can be attributed to the 3d-MT states. For the $Al_{0.0625}V_{0.9375}N$ and $Al_{0.0625}Cr_{0.9375}N$ compounds, the total magnetic moment increases from 2.0 μ_β to 3.0 μ_β. This can be understood as follows: The magnetic moments of $Al_{0.0625}V_{0.9375}N$ and $Al_{0.0625}Cr_{0.9375}N$ are generated by V^{3+} and Cr^{3+} configurations, respectively, and remember that the electronic configurations of V^{3+} =: [Ar]$3d^2$ and Cr^{3+} = [Ar]$3d^3$ happen because the V or Cr atom is located on the Al site. The V or Cr gives three electrons to form the bond; for this reason, the V atom retains two valence electrons and the Cr atom retains three valence electrons. In other words, they have d^2 and d^3 configurations, respectively. These valence electrons couple ferromagnetically, and therefore two and three valence electrons generate 2 μ_β/V-atom and 3.0 μ_β/Cr-atom, respectively. Similar results for the magnetic behavior have been reported for other group III nitride semiconductors such as BN, AlN, and InN in the zincblende structure doped with transition metals, for example Boukra et al. [59] and Espitia et al. [60] in their studies of the $B_{0.9375}Mn_{0.0625}N$ and $B_{0.9375}V_{0.0625}N$ compounds, respectively, while Doumi et al. [61] found the same behavior for $Al_{0.9375}Mn_{0.0625}N$ and $In_{0.9375}Mn_{0.0625}N$ and for $Al_{0.9375}Fe_{0.0625}N$ and $In_{0.9375}Fe_{0.0625}N$, where the magnetic moment is attributed to Mn^{3+}, V^{3+}, and Fe^{3+}. Each transition atom supplies three electrons for bonding.

Due to that $Al_{0.0625}V_{0.9375}N$ and $Al_{0.0625}Cr_{0.9375}N$ in zincblende structure have a half-metallic ferromagnetic behavior, these compounds are promising to be good diluted magnetic semiconductor material with potential applications as spin injector and other applications in spintronic.

CONCLUSIONS

We carry out first-principles calculations of the magnetic properties to low concentration MT (MT = Ti, V, Cr)-doped AlN zincblende namely, $Al_{0.0625}Ti_{0.9375}N$, $Al_{0.0625}V_{0.9375}N$ and $Al_{0.0625}Cr_{0.9375}N$ compounds. Our studies of the band structure and DOS predict a metallic behavior for $Al_{0.0625}Ti_{0.9375}N$ with a magnetic moment of 0.85 μ_β, while that $Al_{0.0625}V_{0.9375}N$ and $Al_{0.0625}Cr_{0.9375}N$ have a half-metallic character, with the majority spin being metallic and the minority spin being semiconductor, with a calculated total magnetic moment of 2.0 μ_β per V atom and 3.0 μ_β per Cr atom. Therefore, $Al_{0.0625}V_{0.9375}N$ and $Al_{0.0625}Cr_{0.9375}N$ is a promising candidate to be a good diluted magnetic semiconductor material.

ACKNOWLEDGEMENTS

The authors are very grateful to the Investigations center of the Universidad Distrital Francisco José de Caldas for its financial support.

REFERENCES

[1] S.C. Jain, M. Willander, J. Narayan, R. Van Overstrateten, J. Appl. Phys. 87 (2000) 965

[2] I. Vurgaftman, J.R. Meyer, L.R. Ram-Mohan, J. Appl. Phys. 89 (2001) 5815.

[3] I. Vurgaftman, J.R. Meyer, J. Appl. Phys. 94 (2003) 3675.

[4] Schupp T, Lischka K., D. J. As, 2010 Journal of Crystal Growth 312 1500

[5] Nakamura S, Senoh M, Iwasa N, Nagahama S, Yamada T and Makai T 1995 Japan. J. Appl. Phys. 34 L1332

[6] Nakamura S 1997 The Blue Laser Diode GaN based Light Emitters and Lasers (Berlin: Springer)

[7] Nakamura S 1999 Semicond. Sci. Technol. 14 R27

[8] W.W. Lei, D. Liu, P.W. Zhu, X.H. Chen, Q. Zhao, G.H. Wen, Q.L. Cui, G.T. Zou, Applied Physics Letters 95 (2009) 162501.

[9] Yao G, Fan G, Xing H, Zheng S, Ma J, Zhang Y and He L 2013 Journal of Magnetism and Magnetic Materials 331 117

[10] Dinh V and Katayama-Yoshida H 2005 ferromagnetism and curie temperature of Vanadium-doped nitrides, Journal of Electron Microscopy 54 (Supplement 1) i61

[11] Espitia M, Díaz J., Castillo L, International Journal of Physical Science 2016 11 11

[12] Q.Y. Wu, Z.Q. Huang, R. Wu, L.J. Chen, Journal of Physics: Condensed Matter 19 (2007) 056209

[13] R. Q. Wu, G. W. Peng, L. Liu , and Y. P. Feng, Z. G. Huang, Q. Y. Wu, Applied Physics Letters **89**, 142501 (2006)

[14] Miguel J. Espitia R, John H. Díaz, César Ortega López, International Journal of Physical Sciences (10)17 (2015): 520-527.

[15] Miguel J.Espitia R, Jonh H. Díaz, Luis Eduardo Castillo, International Journal of Physical Sciences (1)1 (2016) 11-18.

[16] M.J. Espitia Rico, J. H. Díaz F, C. Ortega López, Journal of Physics: Conference Series 687 (2016) 012069

[17] J.H. Díaz F, M.J. Espitia R, J.A. Rodríguez Martínez, Journal of Physics: Conference Series 743 (2016) 012004

[18] R.M. Frazier, J. Stapleton, G.T. Thaler, C.R. Abernathy, S.J. Pearton, R. Rairigh, J. Kelly, A.F. Hebard, M.L. Nakarmi, K.B. Nam, J.Y. Lin, H.X. Jiang, J.M. Zavada, R.G. Wilson, J. Appl. Phys. 94 (2003) 1592.

[19] S.Y. Wu, H.X. Liu, L. Gu, R.K. Singh, L. Budd, M. van Schilfgaarde, M.R. McCartney, D.J. Smith, N. Newman, Applied Physics Letters 82 (2003) 3047.

[20] R.M. Frazier, J. Stepleton, G.T. Thaler, C.R. Abernathy, S.L. Pearton, R. Rairigh, J. Kelly, A.F. Hebard, M.L. Nakarmi, K.B. Nam, J.Y. Lin, H.X. Jiang, J.M. Zavada, R.G. Wilson, Journal of Applied Physics 94 (2003) 1592

[21] D. Kumar, J. Antifakos, M.G. Blamire, Z.H. Barber, Appl. Phys. Lett. 84 (2004) 5004.

[22] Wistrela E, Bittner A, Schneider M Reissner M and Schmid U 2017Jornal of Applied Physics 121 115302.

[23] D. Pan, J. K. Jian, A. Ablat, J. Li, Y. F. Sun, and R. Wu, J. Appl. Phys. 112, 053911 (2012).

[24] Y. Yang, Q. Zhao, X.Z. Zhang, Z.G. Liu, C.X. Zou, B. Shen, D.P. Yu, Applied Physics Letters 90 (2007) 092118

[25] Pearton, Appl. Phys. Lett. 83, 1758 (2003).

[26] K.Y. Ko, Z.H. Barber, M.G. Blamire, J. Appl. Phys. 100 (2006) 083905.

[27] J. T. Luo, Y. Z. Li, X. Y. Kang, F. Zeng, F. Pan, P. Fan, Z. Jiang, and Y. Wang, J. Alloys Compd. 586, 469 (2014).

[28] J. F. Murillo, C. Ortega, M. J. Espitia, Journal of Physics: Conference Series 687 (2016) 012114

[29] Kai Li, Xiaobo Du, Yu Yan, Hongxia Wang, Qing Zhan, Hanmin Jin, Physics Letters A 374 (2010) 3671–3675

[30] J.F. Murillo G, César Ortega López, Miguel J. Espitia R, Results in Physics 5 (2015) 281–285

[31] I. Petrov, E. Mojab, R.C. Powell, J.E. Greene, Appl. Phys. Lett. 60 (1992) 2491

[32] R. Thapa, B. Saha, K.K. Chattopadhyay, Journal of Alloys and Compounds 475 (2009) 373–377

[33] Satoshi Mohri, Tsuyoshi Yoshitake, Takeshi Hara, Kunihito Nagayama, Diamond & Related Materials 17 (2008) 1796–1799

[34] H. Ismail, E. Belloti, K.F. Brennan, J. Kolnik, R. Wang, P.P. Ruden, J. Appl. Phys. 81 (1997) 7827.

[35] O. Ambacher, J. Majewski, C. Miskys, A. Link, M Hermann, M. Eickhoff, M. Stutzmann, F. Bernardini, V. Fiorentini, V. Tilak, B. Schaff, L.F. Eastman, J. Phys.: Condens. Matter 14 (2002) 3399.

[36] C. Mietze, M. Landmann, E. Rauls, H. Machhadani, S. Sakr, M. Tchernycheva, F.H. Julien, W.G. Schmidt, K. Lischka, D.J. As, Phys. Rev. B 83 (2011) 195301.

[37] D.J. As, Microelectron. J. 40 (2009) 204.

[38] J. Simon, N.T .Pelekanos, C. Adelmann, E. Martinez-Guerrero, R.Andre´ , B. Daudin, Le Si Dang, H. Mariette, Phys. Rev. B 68 (2003) 035312.

[39] P. Giannozzi, S. Baroni, N. J. Bonin, a modular and open-source software project for quantum simulations of materials, Condens. Matter, 21 (2009) 395502.

[40] Vanderbilt D, Soft self-consistent pseudopotentials in a generalized eigenvalue formalism, Phys. Rev. B, 41 (1990) 7892.

[41] K. Laasonen, A. Pasquarello, R. Car, C. Lee, D. Vanderbilt, Car-Parrinello molecular dynamics with Vanderbilt ultrasoft pseudopotentials, Phys Rev B, 47 (1993) 10142.

[42] Hohenberg, P., Kohn, W.: Phys. Rev. B 136, 864 (1964)

[43] Kohn, W., Sham, L.J.: Phys. Rev. A 140, 1133 (1965)

[44] J. Perdew, K. Burke, M. Ernzerhof, Generalized Gradient Approximation Made Simple, Physical Review Letter, 77 (1996) 3865.

[45] H. Monkhorst, J. Pack, Special points for Brillouin-zone integrations, Phys Rev B, 13 (1976) 5188.

[46] U.P. Verma, P.S. Bisht, Solid State Sciences 12 (2010) 665–669

[47] A.E. Merad, M.B. Kanoun, J. Cibert, H. Aourag, G. Merad, Materials Chemistry and Physics 82 (2003) 471–477

[48] S. Goumri-Said, M.B. Kanoun, A.E. Merad, G. Merad, H. Aourag, Chem. Phys. 302 (2004) 135

[49] M.B. Kanoun, A.E. Merad, G. Merad, J. Cibert, H. Aourag, Solid-State Electronics 48 (2004) 1601–1606

[50] C. Stampfl, C.G. Van de Walle, Phys. Rev. B 59 (1999) 5521.

[51] Guangrui Yao, Guanghan Fan, Haiying Xing, Shuwen Zheng, Jiahong Ma, Yong Zhang, Longfei He, Journal of Magnetism and Magnetic Materials 331 (2013) 117–121

[52] X.Y. Cui, D. Fernandez-Hevia, B. Delley, A.J. Freeman, C. Stanpfl, Journal of Applied Physics 101 (2004) 103917.

[53] Zhao-Yong Jiao, Shu-Hong Ma, Ji-Fei Yang, Solid State Sciences 13 (2011) 331e336

[54] N.E. Christensen, I. Gorczyca, Phys. Rev. B 50 (1994) 4397

[55] P.E. van Camp, V.E. van Doren, J.T. Devreese, Phys. Rev. B 44 (1992) 9056;

P.E. van Camp, V.E. van Doren, J.T. Devreese, Solid State Commun. 81 (1992)23.

[56] Y. Ohno, D.K. Young, B. Beschoten, F. Matsukura, H. Ohno, D.D. Awschalom, Electrical spin injection in a ferromagnetic semiconductor heterostructure, Nature, 402 (1999) 790

[57] C. Vargas-Hernandez, M. Espitia-Rico M, R. Báez, Half-metallic ferromagnetism of $Zn_xMn_{1-x}O$ compounds: A first-principles study, Computational Condensed Matter, 4 (2015)1-5.

[58] Miguel J. Espitia R, Octavio Salcedo Parra, César Ortega López, Journal of Magnetism and Magnetic Materials 451 (2018) 295–299

[59] A. Boukra A. Zaoui, M. Ferhat. Magnetic trends in GaxMn1-xN, AlxMn1-xN, and InxMn1-xN ternary systems: A first-principles study. JOURNAL OF APPLIED PHYSICS 108, 123904 2010

[60] M.J. Espitia-Rico, J. Díaz, J.A. Martínez. Structural and electronic properties of V-doped cubic BN-A density functional theory study, Solid State Communications, 244 (2016) 23-27

[61] B. Doumi, A. Tadjer, F. Dahmane, D. Mesri , H. Aourag, J. Supercond. Nov. Magn. (2013) 26, 515–525